

Ciliary Muscle Cell Changes During Guinea Pig Development

Andrew D. Pucker,¹ Ashley R. Jackson,² Hugh J. Morris,¹ Andrew J. Fischer,³ Kirk M. McHugh,² and Donald O. Mutti¹

¹College of Optometry, The Ohio State University, Columbus, Ohio, United States

²Center for Molecular and Human Genetics, Nationwide Children's Hospital, Columbus, Ohio, United States

³Department of Neuroscience, The Ohio State University, Columbus, Ohio, United States

Correspondence: Andrew D. Pucker, The Ohio State University, College of Optometry, 320 West 10th Avenue, Columbus, OH 43210-1280, USA; pucker.1@osu.edu.

Submitted: August 11, 2015
Accepted: October 29, 2015

Citation: Pucker AD, Jackson AR, Morris HJ, Fischer AJ, McHugh KM, Mutti DO. Ciliary muscle cell changes during guinea pig development. *Invest Ophthalmol Vis Sci.* 2015;56:7691-7696. DOI:10.1167/iov.15-17927

PURPOSE. Guinea pig ciliary muscle (CM) increases robustly in volume, length, and thickness with age. We wanted to characterize CM cells during development to determine the contributions of hypertrophy (cell size increase) and hyperplasia (cell number increase) during development.

METHODS. Six pigmented guinea pig eyes were collected at each of five ages: 1, 10, 20, 30, and 90 days. Refractive errors and axial lengths were determined. Eyes were temporally marked, enucleated, hemisected, and fixed. Nasal and temporal eye segments were embedded and 30- μ m serial sections were collected; the two most central slides from each hemisection were analyzed with an epifluorescence microscope and Stereo Investigator software to determine normal morphologic parameters.

RESULTS. Refractive errors became less hyperopic ($P = 0.0001$) while axial lengths and CM lengths, cross-sectional areas, volumes, and cell sizes all increased linearly with log age (all $P < 0.00001$). Ciliary muscle cell numbers increased only during the first 20 days of life ($P = 0.02$). Nasal and temporal CM lengths ($P = 0.07$), cross-sectional areas ($P = 0.18$), and cell numbers ($P = 0.70$) were not different, but CM cell sizes were initially larger temporally and became larger nasally after age 30 days.

CONCLUSIONS. The mechanism of guinea pig CM cell growth during the first 90 days of life was characterized by early hyperplasia combined with hypertrophic cell growth throughout development that results in larger CM lengths, cross-sectional areas, and volumes. Nasal-temporal CM development was generally symmetric, but there was more CM hypertrophy nasally at older ages.

Keywords: ciliary muscle, myopia, histology, refractive error, guinea pigs

The ciliary body is an important ocular structure because it produces aqueous humor, controls aqueous humor drainage (uveoscleral outflow), and produces accommodation.¹ The ability to accommodate (changing the eye's refractive focus) results from flexure of the ciliary muscle within the ciliary body.¹ The ciliary muscle runs parallel to the sclera, and its anterior attachment is to the scleral spur/trabecular meshwork while its posterior attachment is to the stroma of the choroid.¹ The ciliary muscle is composed of the circular, radial, and longitudinal fibers.¹ The longitudinal fibers run anterior and parallel to the sclera, and they span the majority of the ciliary body.^{1,2} The circular fibers form an annulus that follows the iris, and they are connected to the longitudinal fibers via the radial fibers.¹ This structural relationship allows the muscle to act as a single functional unit.²

Early work from Woolf³ has documented the general amounts and functional ability of the ciliary muscle in various species (e.g., squirrels, guinea pigs, monkey); however, it was not until the early 1990s that quantitative human ciliary muscle measurements were documented.⁴ Others have since explored how ciliary muscle thicknesses are related to conditions like myopia,⁵⁻⁷ accommodation,⁸⁻¹⁰ and aging,¹¹⁻¹³ and recently the general patterns of ciliary muscle

development were described for the guinea pig.¹¹ Specifically, Pucker et al.¹¹ found with histology that guinea pig ciliary muscle volume increases by approximately 2.5-fold between birth (1 day) and adulthood (90 days). They also determined that ciliary muscle length increases by 48%, ciliary muscle thickness increases by 47%, and ciliary muscle ring diameter increases by 21% during the same time period.¹¹ These data overall indicated that the ciliary muscle primarily grows via length and thickness changes more than through increases in ciliary ring diameter.¹¹

Currently, the processes underlying normal ciliary muscle growth are unknown (e.g., hypertrophy, hyperplasia, or a combination of these processes); therefore, the aim of this investigation was to characterize the cellular changes during postnatal ciliary muscle development. The guinea pig was chosen as the animal model to accomplish this aim because guinea pigs reach adulthood relatively quickly; guinea pigs are able to accommodate, and guinea pigs have a quantifiable amount of ciliary muscle that significantly increases during development.^{11,14,15} Regional ciliary muscle (nasal and temporal) differences were also studied because knowledge of regional guinea pig ciliary muscle differences could prove to be important for future histologic and genetic analyses.

METHODS

Subjects

Seventeen tricolored guinea pigs (*Cavia porcellus*) were bred in-house from Elm Hill Labs (Chelmsford, MA, USA) progenitors. Animals were raised in a 12-hour light/12-hour dark cycle environment. Six eyes were collected at each of five different time points (1, 10, 20, 30, and 90 days) after carbon dioxide asphyxiation. If eyes were incorrectly embedded in optimum cutting temperature (OCT) compound or if eyes were damaged by a microtome malfunction, additional eyes were collected until six high-quality eyes were obtained at each time point. This study adhered to the ARVO Statement for the Use of Animals in Ophthalmic and Vision Research, and The Ohio State University's Institutional Animal Care and Use Committee approved this work (Protocol No. 2012A00000012).

Biometry

Two trained investigators (ADP, DOM) obtained cycloplegic refractive error and axial length measurements with streak retinoscopy and A-scan ultrasound, respectively. In brief, 1% cyclopentolate was applied to each eye, and a second drop was applied to each eye 5 minutes later. Each investigator then performed streak retinoscopy 30 minutes after the instillation of the first drops, and the mean spherical equivalent refractive error from the two investigators was used in analysis. The animals were then anesthetized with 1% to 3% isoflurane, and one drop of 0.5% proparacaine was applied to each eye. A-scan ultrasound (10 MHz, Sonomed 5500; Sonomed Escalon, New Hyde Park, NY, USA) was performed on each eye, and readings were taken until multiple high-quality peaks were visualized. Recordings were then processed to obtain 10 still images from each eye using a frame grabber (EpiPhan Systems, Inc., Palo Alto, CA, USA) and ImageJ software (<http://imagej.nih.gov/ij/>; provided in the public domain by the National Institutes of Health, Bethesda, MD, USA) to calculate axial lengths. Photographs of each eye were also taken, and images were analyzed with ImageJ software as previously described to determine limbal circumference.¹¹

Histology

Ciliary muscle dimensions and cell changes were analyzed with histology.¹¹ Prior to enucleation, the temporal region of each cornea was etched with an inkless tattoo machine. This allowed the investigators to retain each eye's orientation without disrupting the tissue of interest. Each eye was given a code after enucleation to allow for masked analysis. Enucleated eyes were fixed with 4% paraformaldehyde for 1 hour and transferred to 20% sucrose overnight. Eyes were hemisected into nasal and temporal halves and then embedded in OCT compound. Nasal and temporal halves were individually analyzed to determine if there were morphologic differences between the two regions. Care was taken to retain knowledge of each eye's orientation within each block (e.g., corneas were tacked down with a pin and eyes were monitored during the freezing process). Serial 30- μ m-thick sections were collected with microscope slides from each tissue block. After serial sectioning was complete, two representative slides were selected from the center of each slide deck; one section on each of these slides was analyzed. Optimum cutting temperature compound was removed from slides by first heating slides and then washing them with phosphate buffered saline (PBS). Slides were next incubated overnight with an anti- α -smooth muscle actin (SMA) antibody (1:80 dilution, ab5694; Abcam, Cambridge, MA, USA) to

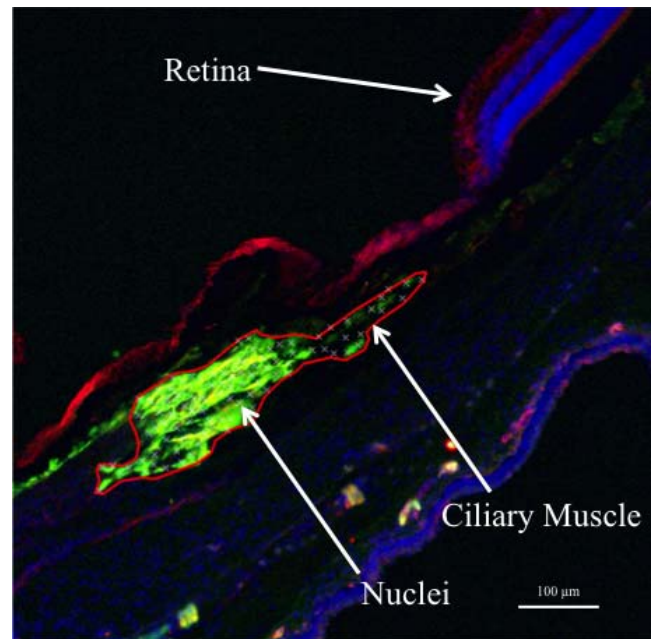


FIGURE 1. Stained 10-day-old guinea pig ciliary muscle ($\times 10$ objective). Note that the border of the muscle is outlined in **bold red**, the smooth muscle fibers are **green**, cell membranes are **red**, and ciliary muscle cell nuclei (**blue**) are labeled with a **white X**.

localize smooth muscle and with an anti-vinculin antibody (1:50 dilution, V4505; Sigma-Aldrich Corp., St. Louis, MO, USA) to localize cell membranes. Slides were then washed with PBS, and they were incubated with a fluorescein isothiocyanate (FITC) (1:500 dilution, ab97199; Abcam) secondary antibody and an Alexa Fluor 568 (1:1000 dilution, A11004; Thermo Fisher Scientific, Waltham, MA, USA) secondary antibody to visualize SMA and vinculin expression, respectively. Draq5 (1:1000 dilution, 62251; Thermo Fisher Scientific) was added at the secondary antibody step to label cell nuclei. Slides were washed again with PBS, mounting medium was added, and coverslips were applied. Representative slides were analyzed as described above without primary antibodies (negative control) to confirm antibody specificity.

Imaging and Analysis

Sections were imaged with a wide-field epifluorescence microscope (DM5000B; Leica Biosystems, Inc., Buffalo Grove, IL, USA) and Leica DC500 digital camera.¹⁶ Slides were first visualized with the $\times 10$ objective to orient the investigator to the sections (Fig. 1), and the $\times 20$ objective was used to obtain images for analysis. High-resolution images (3795 pixels/mm) of each stain were taken and then merged with Adobe Photoshop 6.0 (San Jose, CA, USA) as previously described.¹⁶ All SMA and vinculin images were taken on the same day with the same microscope and camera settings. Draq5 images were taken in a similar manner; however, the camera exposure was varied to allow for the single-nuclei resolution needed for cell counting. Merged images were imported into Stereo Investigator software (MBF Biosciences, Williston, VT, USA) and analyzed. In brief, the ciliary muscle was manually outlined with Stereo Investigator software by tracing the ciliary muscle perimeter using a stylus and touch-screen computer display (Fig. 1); this procedure is repeatable

TABLE 1. Summary of Biometric Measurements

	1 d, Mean \pm SD	10 d, Mean \pm SD	20 d, Mean \pm SD	30 d, Mean \pm SD	90 d, Mean \pm SD
Refractive error, D	+8.85 \pm 1.83	+3.79 \pm 1.50	+1.06 \pm 1.33	+2.56 \pm 1.76	+3.10 \pm 0.84
Axial length, mm	6.28 \pm 0.26	7.04 \pm 0.34	7.19 \pm 0.29	7.92 \pm 0.50	8.28 \pm 0.64
Limbal circumference, mm	16.60 \pm 0.45	19.17 \pm 0.58	19.32 \pm 0.30	20.31 \pm 0.87	22.03 \pm 0.63

to within $\pm 0.012 \text{ mm}^2$.¹¹ Stereo Investigator uses this information to determine both ciliary muscle cross-sectional area and ciliary muscle length. Mean SMA brightness was recorded from Stereo Investigator after correcting for background brightness by analyzing only the green channel images (unmerged image); unmerged images were required because Stereo Investigator was unable to uncouple the brightness values obtained from the multichannel images. Smooth muscle actin brightness was used as a measure of the overall concentration of smooth muscle present. Numbers of cell nuclei were obtained from Stereo Investigator using optimized cell nuclei size detection parameters (Fig. 1). Mean values for each eye were then used to calculate cell area (cross-sectional area / mean cell number) and ciliary muscle volume (cross-sectional area \times limbal circumference).¹¹ Nasal and temporal ciliary muscle cross-sectional areas, lengths, cell numbers, and cell area differences were determined by comparing the corresponding regions of each eye. Representative confocal microscopy images were also obtained with a Zeiss LSM 510 (Pleasanton, CA, USA) confocal microscope and ZEN 2009 software to determine if ciliary muscle cells were mono- or multinuclear.

Statistical Analysis

Statistical calculations were made with Microsoft Excel (Redmond, WA, USA) and Stata 13.0 software (StataCorp LP, College Station, TX, USA), and all statistical analyses were performed with individual data points rather than with group means. Linear regression was used to analyze refractive error, axial length, cross-sectional area, cell number, and mean cell area as a function of \log_{10} age. Log age was used in both regression and graphical analysis because our past work has indicated that this function produced the strongest best-fit lines.¹¹ The Kruskal-Wallis (KW) test was used to determine the ages at which cell number was significantly different from that at 1 day

old. The Wilcoxon signed-rank test (WS) was used to compare nasal and temporal differences. Tests were considered significant when $P < 0.05$.

RESULTS

Mean refractive error started off highly hyperopic in the 1-day age group ($+8.85 \pm 1.83$ diopters [D]) but was far less hyperopic in the 90-day age group ($+3.10 \pm 0.84$ D; $P < 0.00001$; Table 1). A pairwise comparison showed that refractive error significantly decreased with log age from both 1 to 10 days ($P = 0.004$) and 10 to 20 days ($P = 0.025$) of age; however, no significant decreases were seen after these time points. Both mean axial length (6.28 ± 0.26 – 8.28 ± 0.64 mm) and limbal circumference (16.60 ± 0.45 – 22.03 ± 0.63 mm) were significantly larger in the older compared to the younger animals ($P < 0.00001$; Table 1). Refractive error, axial length, and limbal circumference were all in general agreement with past studies.^{11,15}

Wide-field microscopy analysis found no specific staining on negative control slides (not shown). Ciliary muscle cross-sectional areas (0.038 ± 0.002 – $0.078 \pm 0.011 \text{ mm}^2$), ciliary muscle lengths (416.6 ± 37.4 – $793.3 \pm 74.9 \text{ }\mu\text{m}$), and ciliary muscle volumes (0.62 ± 0.04 – $1.72 \pm 0.21 \text{ mm}^3$) all showed significant linear relationships with log age (all $P < 0.00001$; Figs. 2, 3, 4). Confocal microscopy indicated that guinea pig ciliary muscle cells were mononuclear and that all three labels were specific for their regions of interest (Fig. 5). Ciliary muscle cell size linearly increased with log age (244.3 ± 25.8 – $409.7 \pm 80.2 \text{ }\mu\text{m}^2$; $P < 0.00001$) over the range of ages of the study (Fig. 6). The number of ciliary muscle cells showed a linear relationship with log age ($P = 0.048$); however, there were significantly more cells only at 20 and at 90 days of age compared to 1 day of age (154.4 ± 12.3 cells compared to 194.2 ± 27.7 and 193.8 ± 31.0 cells; $P = 0.02$) (Fig. 7). The

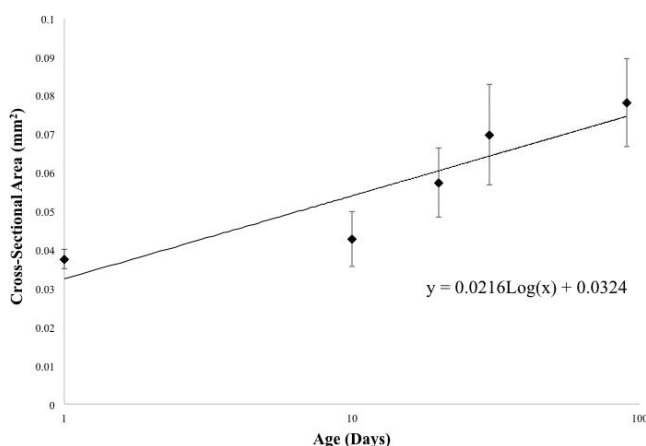


FIGURE 2. Mean ciliary muscle cross-sectional area during development.

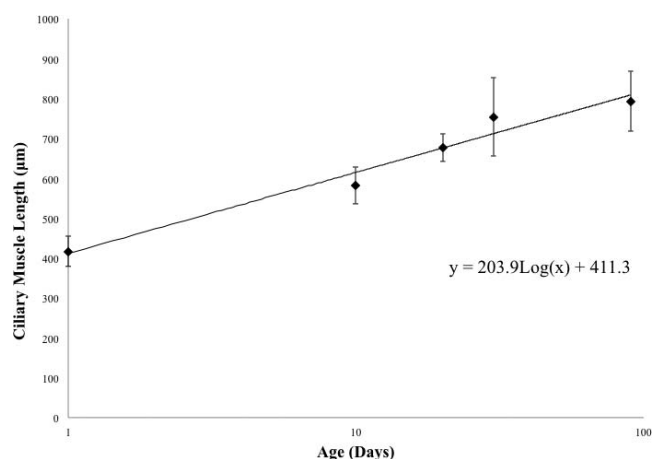


FIGURE 3. Mean ciliary muscle length during development.

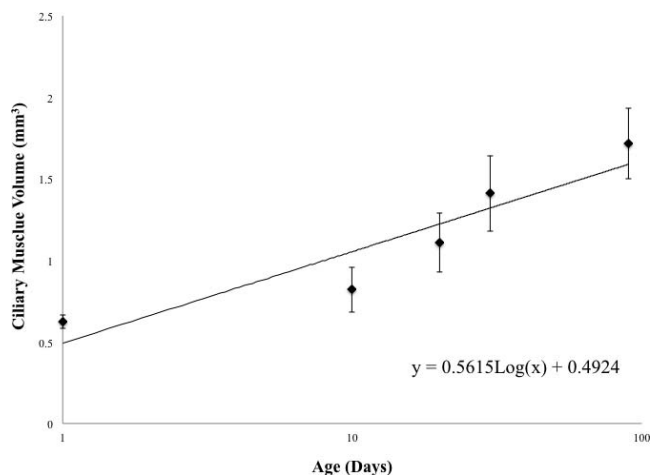


FIGURE 4. Mean ciliary muscle volume during development.

overall mean SMA brightness (40.3 ± 8.3 units) did not significantly change with log age ($P = 0.06$), which indicates that a greater amount of SMA filaments must be added during this time period in order to maintain the same SMA brightness over a greater cross-sectional area (Fig. 8).

Ciliary muscle nasal and temporal comparisons showed that, in general, ciliary muscle lengths ($P = 0.07$), cross-sectional areas ($P = 0.18$), and cell numbers ($P = 0.70$) were not regionally different (Table 2). Cell size had a significant interaction between age and ciliary muscle region ($P = 0.02$), which indicates that the difference between nasal and temporal ciliary muscle cell sizes varied by age. Analysis with WS indicated that ciliary muscle cells were significantly

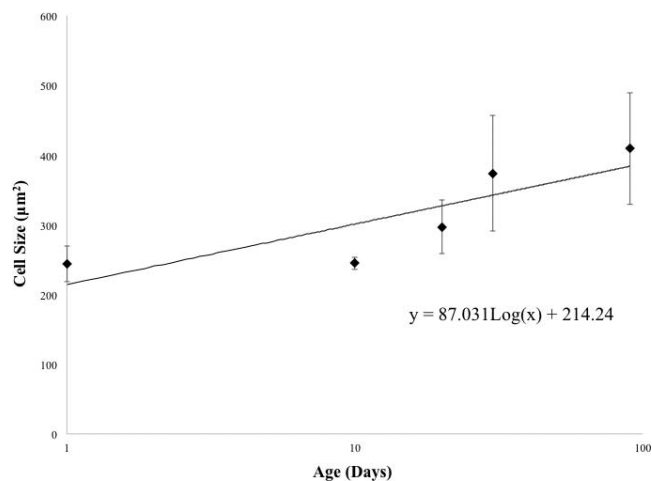


FIGURE 6. Mean ciliary muscle cell size during development.

larger temporally at 1 day of age ($P = 0.027$), but they became significantly larger nasally by 30 days of age ($P = 0.027$).

DISCUSSION

The ciliary muscle undergoes several major changes during normal guinea pig development. Specifically, this study found that the number of cells within a guinea pig's ciliary muscle increases by approximately 26% during the first 20 days of life, which was followed by stability in cell numbers. Ciliary muscle cell size increased by 1.68 times and ciliary muscle volume increased by 2.75 times while SMA brightness did not significantly change during the first 90 days of life. Neverthe-

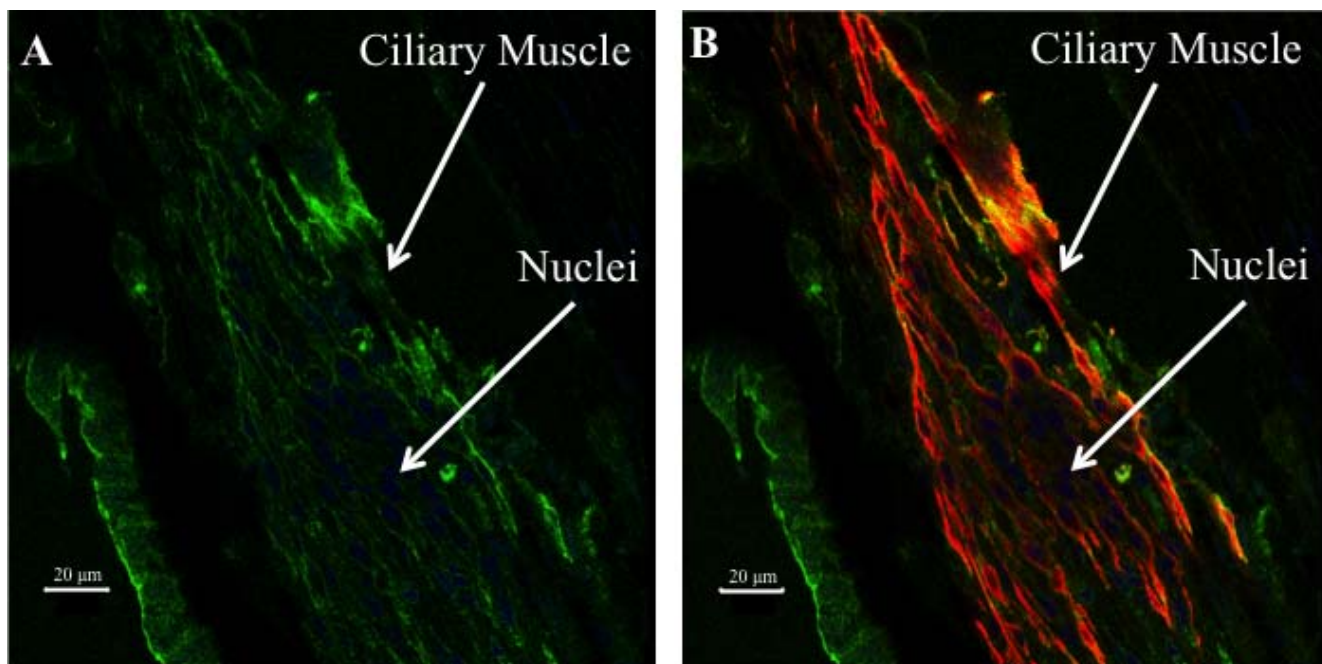


FIGURE 5. Confocal microscopy images of a 1-day-old guinea pig ciliary muscle ($\times 40$ objective). Red stain (smooth muscle actin) is a marker for ciliary muscle fibers, green stain (vinculin) is a marker for cell membranes, and blue stain (Draq5) is a marker for cell nuclei. Image (A) is a merged image of the green and blue colors while image (B) is a merged image of all three colors.

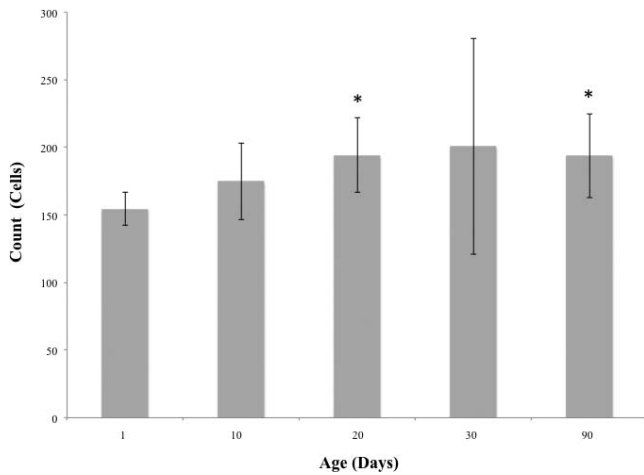


FIGURE 7. Mean ciliary muscle cell number during development. Asterisk indicates time points with significant increase ($P < 0.05$) in cell numbers compared to baseline.

less, SMA brightness did have a trend toward decreased brightness over time with a marginal P value of 0.06; a larger sample size would be needed to evaluate this association in more detail. These data suggest that the normal guinea pig ciliary muscle grows via hyperplasia (increased cell number) during the first 20 days of life and via hypertrophy (larger cells with more muscle filaments) during the first 90 days of life.

This study also characterized how the ciliary muscle cell morphology changes over time in pigmented guinea pigs. Dimensions showed a similar relationship with log age, but with different values compared to our past work with albino guinea pigs.¹¹ The current study found that 1-day-old pigmented guinea pigs had mean ciliary muscle lengths of 416.6 μm , cross-sectional areas of 0.04 mm^2 , and volumes of 0.62 mm^3 while we have previously found that that 1-day-old albino guinea pigs had mean ciliary muscle lengths of 625.0 μm , cross-sectional areas of 0.02 mm^2 , and volumes of 0.40 mm^3 .¹¹ The same relationship was seen with the larger ciliary muscles in the 90-day age groups. Therefore, with the exception of length, a pigmented guinea pig's ciliary muscle appears to be larger on average than an albino guinea pig's ciliary muscle. It is possible that the above ciliary muscle length differences can be explained by the pigmented eyes being shorter axially than the albino eyes.¹¹ The above difference may also exist because the Elm Hill Labs guinea

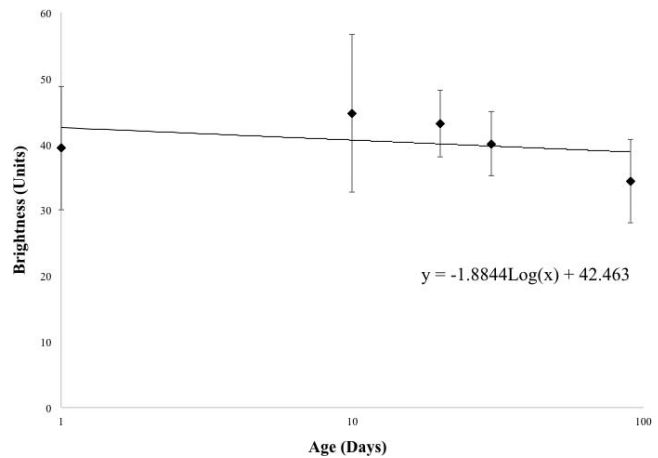


FIGURE 8. Smooth muscle actin brightness during development.

pigs used in this experiment seem to be resistant to experimental myopia and may have a slightly different growth pattern than the other existing guinea pig strains (Garcia M, et al. *IOVS* 2015;ARVO E-Abstract 2167); therefore, ciliary muscle growth patterns should be tested in other guinea pig strains and other animal models to determine the generalizability of our results. Within-strain controls will also be important when comparing the effects of induced myopia on the ciliary muscle. While it is possible that the different tissue fixation and staining methods that were used in these two experiments could have produced histologic artifacts, the above data suggest that pigmented animals may be more useful for studying the ciliary muscle than albino animals because pigmented animals have more overall ciliary muscle to analyze.

In addition to guinea pig ciliary muscle strain variations, ciliary muscle analysis is also complicated by the fact that mammalian ciliary muscle is made of atypical smooth muscle (e.g., embryologically derived from neural crest instead of mesoderm as with most muscle) that has some skeletal muscle properties (e.g., voluntary movement).^{1,3,17} This structure is further complicated by the fact that ciliary muscle appearance and function vary among species (e.g., birds have a skeletal muscle-based ciliary muscle [striate and multinuclear] while mammals have a smooth muscle-based ciliary muscle [nonstriated and mononuclear]).^{3,18,19} Therefore, we confirmed with confocal microscopy that the guinea

TABLE 2. Comparison of Nasal and Temporal Ciliary Muscle Differences

	Nasal Region, Mean \pm SD	Temporal Region, Mean \pm SD	P Value	Interaction Between Region and Age, P Value*
Ciliary muscle length, μm	630.0 \pm 149.6	657.9 \pm 158.0	$P = 0.07$	
Ciliary muscle cross-sectional area, mm^2	0.059 \pm 0.022	0.055 \pm 0.018	$P = 0.18$	
Ciliary muscle cell number, cells	178.0 \pm 48.8	187.8 \pm 60.5	$P = 0.70$	
Ciliary muscle cell size, $\mu\text{m}^2/\text{cell}$	346.5 \pm 143.4	294.2 \pm 52.6		
Age group, d				
1	230.8 \pm 19.3	263.4 \pm 40.4		$P = 0.028$
10	250.8 \pm 33.4	247.0 \pm 17.1		$P = 0.75$
20	315.2 \pm 78.2	290.1 \pm 26.2		$P = 0.46$
30	424.6 \pm 109.9	322.2 \pm 57.9		$P = 0.028$
90	511.4 \pm 188.6	348.1 \pm 49.0		$P = 0.046$

Values are means across ages unless age is noted.

* A Wilcoxon signed-rank comparison between regions at a given age.

pig's ciliary muscle was mononuclear in order to validate our ciliary muscle cell size and cell counting measurement approaches. While these data help justify our cell size analysis method, our method should still be seen as a relative estimate by age because individual cell dimensions were not quantified and some noncellular areas were included in our final calculations (e.g., histologic tissue separation). However, these measurement issues were similar across all samples. Our method was also more feasible than quantifying hundreds of individual cells in each sample.

This study also compared nasal and temporal ciliary muscle regions because regional differences have been previously found in birds, and knowledge of regional differences could be important for future histologic and genetic analyses of intereye differences.¹⁹ In general, we found that most nasal and temporal parameters analyzed were similar; however, mean ciliary muscle cell size was found to be larger temporally at the 1-day time point and larger nasally at the 30-day time point, which indicates that the nasal cells have a more robust growth pattern than temporal cells. These data also suggest that one should be mindful of a rodent's eye orientation when analyzing the ciliary muscle.

In summary, this work determined that the overarching mechanism of ciliary muscle growth is biphasic during normal guinea pig development. The ciliary muscle initially undergoes a combined hyperplastic/hypertrophic phase for the first 20 days of life, and it switches to a simple hypertrophic phase for days 20 through 90. The study also provides the necessary normative data needed for future experiments that focus on determining the mechanisms by which the ciliary muscle becomes thicker in myopic subjects. In addition, our data suggest that there may be significant strain-specific differences in the overall size and composition of the ciliary muscle. Overall, it is hoped that this work serves to help establish the guinea pig as an animal model for studying ciliary muscle-related conditions (e.g., myopia, accommodation),⁵⁻¹⁰ and that the findings described in this manuscript will lead to a better understanding of how ciliary muscle development might influence these conditions.

Acknowledgments

Supported by National Institutes of Health/National Eye Institute Grant K08EY023264 and the E.F. Wildermuth Foundation. The authors alone are responsible for the content and writing of the paper.

Disclosure: **A.D. Pucker**, Johnson & Johnson Vision Care, Inc. (F); **A.R. Jackson**, None; **H.J. Morris**, None; **A.J. Fischer**, None; **K.M. McHugh**, None; **D.O. Mutti**, None

References

1. Remington LA. *Clinical Anatomy of the Visual System*. 2nd ed. St. Louis: Butterworth-Heinemann; 2005:44-47.

2. Ebersberger A, Flugel C, Lutjen-Drecoll E. Ultrastructural and enzyme histochemical studies of regional structural differences within the ciliary muscle in various species [in German]. *Klin Monbl Augenbeilkd*. 1993;203:53-58.
3. Woolf D. A comparative cytological study of the ciliary muscle. *Anat Rec*. 1956;124:145-163.
4. Tamm S, Tamm E, Rohen JW. Age-related changes of the human ciliary muscle. A quantitative morphometric study. *Mech Ageing Dev*. 1992;62:209-221.
5. Oliveira C, Tello C, Liebmann JM, Ritch R. Ciliary body thickness increases with increasing axial myopia. *Am J Ophthalmol*. 2005;140:324-325.
6. Bailey MD, Sinnott LT, Mutti DO. Ciliary body thickness and refractive error in children. *Invest Ophthalmol Vis Sci*. 2008;49:4353-4360.
7. Pucker AD, Sinnott LT, Kao CY, Bailey MD. Region-specific relationships between refractive error and ciliary muscle thickness in children. *Invest Ophthalmol Vis Sci*. 2013;54:4710-4716.
8. Drexler W, Findl O, Schmetterer L, Hitzenberger CK, Fercher AF. Eye elongation during accommodation in humans: differences between emmetropes and myopes. *Invest Ophthalmol Vis Sci*. 1998;39:2140-2147.
9. Lewis HA, Kao CY, Sinnott LT, Bailey MD. Changes in ciliary muscle thickness during accommodation in children. *Optom Vis Sci*. 2012;89:727-737.
10. Lossing LA, Sinnott LT, Kao CY, Richdale K, Bailey MD. Measuring changes in ciliary muscle thickness with accommodation in young adults. *Optom Vis Sci*. 2012;89:719-726.
11. Pucker AD, Carpenter AR, McHugh KM, Mutti DO. Guinea pig ciliary muscle development. *Optom Vis Sci*. 2014;91:730-739.
12. Nishida S, Mizutani S. Quantitative and morphometric studies of age-related changes in human ciliary muscle. *Jpn J Ophthalmol*. 1992;36:380-387.
13. Pardue MT, Sivak JG. Age-related changes in human ciliary muscle. *Optom Vis Sci*. 2000;77:204-210.
14. Ostrin LA, Garcia MB, Choh V, Wildsoet CF. Pharmacologically stimulated pupil and accommodative changes in Guinea pigs. *Invest Ophthalmol Vis Sci*. 2014;55:5456-5465.
15. Howlett MH, McFadden SA. Emmetropization and schematic eye models in developing pigmented guinea pigs. *Vision Res*. 2007;47:1178-1190.
16. Fischer AJ, Zelinka C, Milani-Nejad N. Reactive retinal microglia, neuronal survival, and the formation of retinal folds and detachments. *Glia*. 2015;63:313-327.
17. Gage PJ, Rhoades W, Prucka SK, Hjalt T. Fate maps of neural crest and mesoderm in the mammalian eye. *Invest Ophthalmol Vis Sci*. 2005;46:4200-4208.
18. Glasser A, Murphy CJ, Troilo D, Howland HC. The mechanism of lenticular accommodation in chicks. *Vision Res*. 1995;35:1525-1540.
19. Murphy CJ, Glasser A, Howland HC. The anatomy of the ciliary region of the chicken eye. *Invest Ophthalmol Vis Sci*. 1995;36:889-896.